RASĀYAN *J. Chem.*
Vol. 19 | Special Issue | 223-231 | 2026
ISSN: 0974-1496 | e-ISSN: 0976-0083 | CODEN: RJCABP
http://www.rasayanjournal.com
http://www.rasayanjournal.co.in

SUSTAINABLE SYNTHESIS OF *Citrus Limon*-MEDIATED TiO_2 NANOPARTICLES FOR OPTIMIZED PHOTOCATALYTIC DEGRADATION OF METHYLENE BLUE

S. S. Vanjarana[1,✉] and C. B. Nalluri[2]
[1]Department of Chemical Engineering, B. V. Raju Institute of Technology, Narsapur-502313, (Telangana) India
[2]Department of Chemical Engineering, Andhra University College of Engineering(A), Visakhapatnam-530002 (Andhra Pradesh) India
✉Corresponding author: sravanisameera92@gmail.com

ABSTRACT
The implementation of processes imitating natural systems might be necessary to ensure sustainability. Titanium dioxide (TiO_2) nanoparticles were synthesized in an eco-friendly manner using *citrus limon* leaf extract as both a reducing and stabilizing agent. X-ray diffraction (XRD), field-emission scanning electron microscopy (FESEM), Fourier-transform infrared spectroscopy (FTIR) and energy-dispersive spectroscopy (EDS) were used to characterize the synthesized nanoparticles. The crystallized material was in the anatase phase, was quasi-spherical, with slight agglomeration and had distinct Ti–O–Ti vibration bands. The synthesized TiO_2 nanoparticles were assessed for their photocatalytic activity by UV light-induced methylene blue (MB) degradation. The effects of catalyst loading (0.1–0.3 g L^{-1}), initial dye concentration (10–50 ppm) and irradiation time (5–180 min) were examined. With the optimum conditions, about 85.36% MB removal was accomplished. The degradation process was a pseudo-first-order reaction with the rate constant of 0.0124 min^{-1}, (R^2= 0.9839). The response surface methodology (RSM) using central composite design (CCD) generated a statistically significant quadratic model with a high value of R^2 (99.69%) and a low p-value (< 0.0001), showing good predictive capacity. The study has shown the potential of plant-mediated TiO_2 nanoparticles as a simple, environmentally friendly and promising photocatalyst for treating the wastewater containing dyes. The integration of bio-derived synthesis with photocatalytic wastewater treatment adds to the avenues for more sustainable environmental remediation, while paving the way for optimization and scaling up of plant-assisted nanomaterial synthesis and photocatalytic processes. The study is closely related with SDG-6 (Clean Water and Sanitation) because of its concern with the target of removing the organic dye pollutants from wastewater. In addition, the study is related to the scope of the Special Issue, investigating sustainable materials, eco-friendly synthesis strategies, and cutting-edge photocatalytic processes for environmental cleanup.

Keywords: Sustainable Synthesis, Titania (Tio_2) Nanoparticles, *Citrus Limon* Leaf Extract, Photocatalysis, Methylene Blue Degradation, Response Surface Methodology.

RASĀYAN *J. Chem.*, Thematic Issue, 2026

INTRODUCTION

The release of dye-containing effluents from industrial processes is one of the major environmental issues associated with synthetic dyes, as they could negatively affect the photosynthetic process and aquatic life, and could also affect the light penetration in receiving water bodies. They are hard to treat with traditional biological methods due to their persistence and complex chemistry. Therefore, the removal and degradation of synthetic dyes from wastewater through efficient, economical and sustainable technologies are important research fields in environmental science. Heterogeneous photocatalysis has recently been shown to be a promising advanced treatment method for the degradation of persistent organic pollutants in wastewaters.[1-3] Methylene blue (MB) is a widely used cationic dye in textile, paper, and related industries. Its stable molecular structure makes it a common model pollutant in photocatalytic degradation research.[4-5] Advanced oxidation processes (AOPs) have proven to be an efficient method to degrade and, under proper conditions, mineralize this kind of recalcitrant organic contaminants by producing highly reactive oxygen species (ROS) such as hydroxyl radicals (HO•). Titanium dioxide (TiO_2) has been widely studied as a semiconductor photocatalyst due to its strong oxidizing power, chemical stability, relatively

This work is licensed under a CC BY 4.0 license.

low cost, and UV photocatalytic activity. In particular, anatase is an appealing type for photocatalytic application because of its appropriate electronic structure and high photocatalytic activity under UV illumination. The treatment of dyes and other organic contaminants in wastewater by the use of TiO_2-based photocatalysis is still a research area of interest as indicated by recent reviews.[6–8] The traditional techniques for synthesizing TiO_2 nanoparticles are sol–gel, hydrothermal, precipitation, and others chemical processes. Multiple processing steps, high temperatures, use of organic solvents, or other chemical reagents are among the limitations that have spurred growing interest in biological and plant-mediated synthesis processes, where the particle's reduction and nucleation, as well as stabilization and surface modification, can involve naturally occurring phytochemicals.[6,9] These limitations have encouraged increasing interest in biological and plant-mediated synthesis routes, in which naturally occurring phytochemicals can participate in the reduction, nucleation, stabilization, and surface modification of nanoparticles. Such approaches can simplify synthesis and reduce dependence on conventional chemical reagents, thereby supporting more environmentally responsible nanomaterial production. Recent reviews have emphasized the growing application of plant-mediated TiO_2 nanoparticles for dye-contaminated water treatment.[9,10] For example, TiO_2 nanoparticles synthesized using plant-derived materials have demonstrated photocatalytic activity toward different dyes, while recent studies using plant or agro-waste extracts have further demonstrated the potential of these approaches for sustainable photocatalyst preparation.[11–14] *Citrus limon* is a readily available plant resource containing phytochemicals such as organic acids, flavonoids, and polyphenolic compounds that can participate in nanoparticle formation and stabilization. The use of *Citrus limon* extracts for TiO_2 synthesis has recently been investigated, demonstrating the feasibility of employing its phytochemical constituents in the preparation of photocatalytically active TiO_2 nanoparticles.[15] However, the photocatalytic performance of a synthesized nanomaterial depends not only on its structural and surface characteristics but also on operating variables such as catalyst dosage, initial pollutant concentration, irradiation time, and their interactions. Therefore, optimization of the photocatalytic process is essential for identifying suitable operating conditions and improving the practical applicability of the treatment process. When compared to traditional one-factor-at-a-time approaches, response surface methodology (RSM) offers a systematic statistical strategy for assessing the impacts of several process factors and their interactions while requiring fewer experimental trials. Central composite design (CCD), one of the commonly used RSM designs, has been applied to optimize photocatalytic degradation processes involving TiO_2-based catalysts and dye pollutants.[16,17] More recent studies have also demonstrated the value of combining TiO_2-based photocatalysis with statistical or computational optimization for improving pollutant degradation and identifying favorable operating conditions.[13,16] Nevertheless, comparatively limited studies have integrated a *Citrus limon*-mediated TiO_2 synthesis route with systematic RSM-CCD optimization of multiple operational variables for MB photodegradation. This represents an important research gap because linking sustainable nanoparticle synthesis with statistical process optimization can provide a more systematic basis for improving photocatalytic treatment efficiency and reducing experimental requirements. Therefore, employing *Citrus limon* leaf extract as a plant-derived reducing and stabilizing medium, the current study explores the sustainable production of TiO_2 nanoparticles and assesses their photocatalytic efficacy for the successful degradation of MB under UV irradiation. The synthesised TiO_2 nanoparticles were characterised by X-ray diffraction (XRD), field-emission scanning electron microscopy (FESEM), Fourier-transform infrared spectroscopy (FTIR), and energy-dispersive spectroscopy (EDS), confirming their structural, morphological, functional, and elemental features. XRD showed the crystalline phases, FESEM revealed the surface morphology, FTIR identified the functional groups, and EDS confirmed the elemental composition. The effects of initial MB concentration, catalyst dosage, and irradiation time were systematically investigated, and their individual and interactive effects on MB degradation were evaluated using RSM based on a CCD. The specific research gap addressed by this work is the integration of plant-mediated *C. limon*/TiO_2 synthesis with multivariable statistical optimization of MB photodegradation. This approach provides insights into the relationship between operating parameters and photocatalytic performance and establishes optimized conditions that may support the further development and scale-up of sustainable photocatalytic wastewater treatment. The ecological significance of this research aligns with the United Nations Sustainable Development Goal 6

(SDG 6: Clean Water and Sanitation), especially Target 6.3, which advocates for enhancing water quality through pollution reduction and the minimization of dangerous substances, while increasing the safe treatment and reuse of wastewater.[18] By combining a plant-mediated synthesis route with photocatalytic degradation of an organic dye pollutant, the present study contributes to the development of environmentally responsible approaches for wastewater treatment and water-quality improvement.

EXPERIMENTAL

Materials and Methods

Fresh *Citrus limon* leaves were thoroughly washed with deionised water to remove dust and other impurities and then dried in the shade to remove water on the surface. Approximately 20 g of finely chopped leaves were boiled in 100 mL of deionized water for 30 min. The resulting mixture was then left to cool down to room temperature and then filtered using the Whatman No. 1 filter paper to get the aqueous leaf extract. The filtrate was stored at 4 ^{o}C for further use in nanoparticle synthesis. The precursor used in the synthesis of TiO_2 was titanium isopropoxide (TIP, 97% purity). A volumetric proportion of TIP, *Citrus limon* leaf extract and distilled water was mixed in a volumetric ratio of 1:1:5. To allow the hydrolysis and condensation reactions, the reaction mixture was kept at 80 ^{o}C. The mixture slowly assumed a milky white hue, which was a sign of the development of TiO_2 precursor particles. The resultant precipitate was separated by filtration, and the resulting suspension was dried. The material was then calcined at 400 ^{o}C in a muffle furnace to get crystalline TiO_2 nanoparticles.[11] Fig.-1 represents the schematic diagram of the TiO_2 nanoparticle synthesis process via plant leaves.

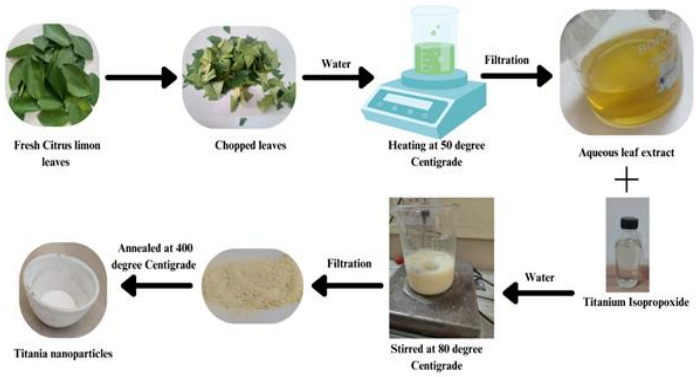


Fig.-1: Schematic Representation of the Plant-Mediated Synthesis of TiO_2 Nanoparticles

The XRD (λ = 1.5406 Å) study was carried out to study the crystalline nature of the synthesised material. The morphology and elemental constituents were determined using FESEM and EDS, respectively. The obtained FT-IR spectra ranged from 4000 to 500 cm^{-1} for identification of the surface functional groups. The photocatalytic efficacy was evaluated by examining the degradation of methylene blue under UV light. Before each run, to attain adsorption-desorption equilibrium, the suspension was agitated in the dark for 30 minutes. Catalyst loading (0.1–0.3 g L^{-1}), initial MB concentration (10–50 ppm), and irradiation time (5–180 min) were varied systematically. The residual dye concentration was quantified using spectrophotometry at 664 nm after aliquots removed at predetermined intervals were centrifuged to extract the catalyst. The efficiency was calculated based on the change in dye concentration using Equation (1).

$$\text{Efficiency}(\%) = \frac{C_{initial} - C_{final}}{C_{initial}} \times 100 \quad (1)$$

Here, $C_{initial}$ and C_{final} are the MB concentrations at time 0 minutes and irradiation time t, respectively.

The three process variables were optimized using a CCD within the scope of the RSM. A quadratic regression model was fitted to the experimental data, and its statistical validity was confirmed using analysis of variance. The optimum conditions were identified as those that maximised the predicted degradation efficiency.

RESULTS AND DISCUSSION

XRD Analysis

In Fig.-2(a), the diffraction pattern exhibited the characteristic reflections of the anatase phase, with the most intense peak observed at 2θ = 25.37°, corresponding to the (101) crystallographic plane. Other characteristic reflections were observed at 37.90°, 48.13°, 54.55°, and 62.70°, corresponding to the (004), (200), (105), and (204) planes, respectively. The anatase structure of TiO_2 is compatible with these reflections. The Debye-Scherrer equation yielding an average crystallite size of about 4.5 nm, with a range from 3.40 to 6.53 nm. The absence of additional diffraction peaks attributable to secondary crystalline phases indicates the production of mostly phase-pure anatase TiO_2. The observed anatase structure is favourable for photocatalytic applications because of its established photocatalytic activity under UV irradiation.[12]

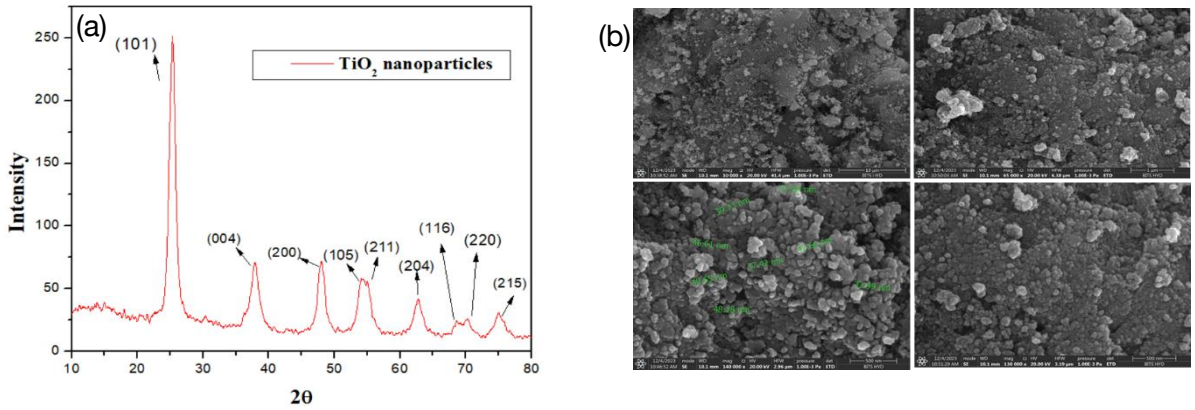


Fig.-2: (a) XRD Graph and (b) SEM images of TiO_2 Nanoparticles

Morphological Analysis

The FESEM image of the synthesized TiO_2 nanoparticles is shown in Fig.-2(b). The particles are mainly quasi-spherical, and the particle sizes range from approximately 15 to 40 nm. Some degree of agglomeration is evident, which is commonly observed in nanoparticles during drying and calcination because of the high surface energy of nanosized particles. The particle size observed by FESEM is larger than the crystallite size estimated from XRD. This difference is expected because a single particle observed by FESEM may consist of several crystallites. The relatively uniform morphology and limited agglomeration may be associated with the presence of phytochemical constituents in the *Citrus limon* leaf extract, which can interact with the precursor species during nanoparticle formation and influence particle growth and stabilization.[11,12]

FTIR Analysis

According to the FTIR pattern in Fig.-3(a), O–H stretching vibrations associated with adsorbed moisture and surface hydroxyl groups are primarily responsible for a broad absorption band centred at roughly 3369 cm^{-1}. The band at 1634 cm^{-1} is associated with the bending vibration of molecular water. Weak bands observed near 2339 and 2108 cm^{-1} may be associated with atmospheric CO_2 and/or residual organic species originating from the plant extract. The prominent absorption bands at 621.64 and 669.52 cm^{-1} are attributed to Ti–O–Ti vibrations, confirming the formation of the TiO_2 lattice. The presence of residual organic-related bands suggests that phytochemical constituents from the *Citrus limon* extract may have remained associated with the nanoparticle surface following synthesis and calcination.[12]

EDS Analysis

The EDS spectrum (Fig.-3b) indicated the presence of titanium (54.09 wt.%) and oxygen (29.85 wt.%). Some residual organics, typical of plants, were thought to be adsorbed on the particle surface, and this was the reason for the minor carbon signal.[13]

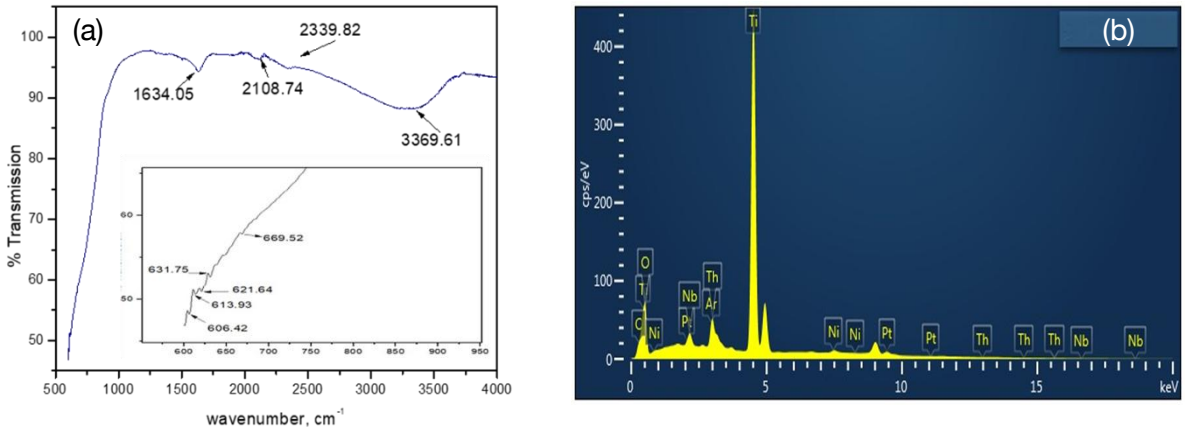


Fig.-3: (a) FTIR Plot and (b) EDX Plot of TiO_2 Nanoparticles

Photocatalytic Degradation Performance

The green-synthesized TiO_2 was effective in degrading methylene blue under the UV light. The initial dye concentration and catalyst dosage were found to have less impact on efficiency than did the irradiation time, which was represented in Figs.-4 and 5. Using extended illumination, continuous generation of ROS was obtained leading to progressive dye oxidation. Beyond this optimal duration, the increase in degradation was relatively small because a substantial fraction of MB had already been degraded.[14] An increase in catalyst concentration led to an increase in the number of active sites and thus to a better degradation performance, but this effect became weaker at higher loadings due to an increase in particle aggregation and turbidity, which decreased the penetration of photons.[15] Lower initial MB concentrations yielded higher removal efficiencies, reflecting an excess of surface sites relative to dye molecules. At elevated dye levels, competition for active sites and diminished light transmission through the suspension lowered the observed efficiency.[16,23] Overall, the maximum performance arises from the combined optimisation of irradiation time, catalyst dosage, and dye concentration.

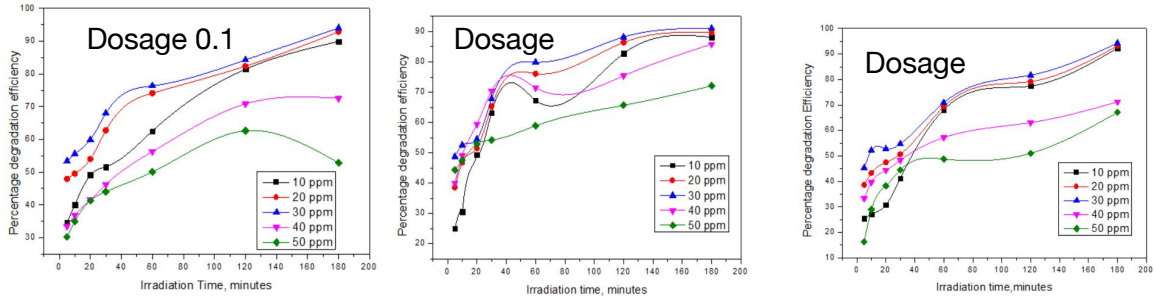


Fig.-4: The Impact of Irradiation Time on Degradation Efficiency for 0.1, 0.2 and 0.3g/L Catalyst Dosage

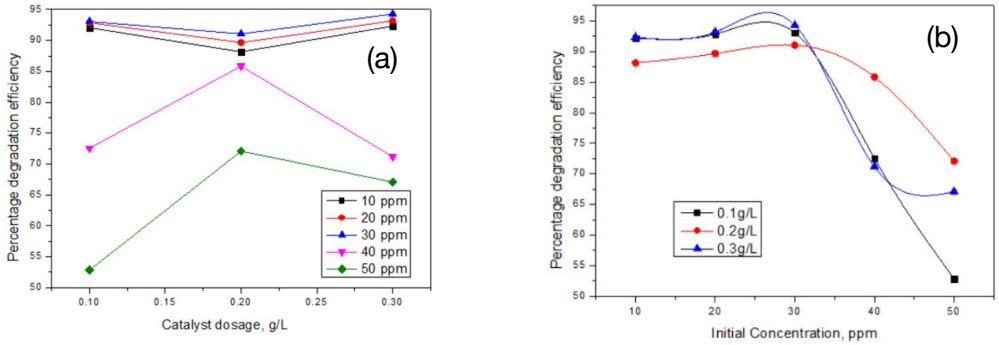


Fig.-5: The Impact of Catalyst Dosage (a) and initial MB Concentration (b) on Degradation Efficiency

Kinetic Study of Photocatalytic Degradation

The experimental degradation data were evaluated using pseudo-first-order and pseudo-second-order kinetic models, as shown in Fig.-6(a) and (b). The pseudo-first-order model gave a higher coefficient of determination than the pseudo-second-order model, indicating that the experimental degradation data were better described by pseudo-first-order kinetics under the investigated conditions. The pseudo-first-order model had an apparent rate constant of 0.0124 min^{-1} and R^2 value of 0.9839. The pseudo-first-order model exhibited a superior fit, which is consistent with the commonly observed kinetic behaviour of heterogeneous photocatalytic degradation systems at relatively low pollutant concentrations.[17] The apparent rate constant obtained in this study provides a quantitative measure of the degradation rate under the experimental conditions and can be used for comparison with other photocatalytic systems, provided that the operating conditions are comparable.[17]

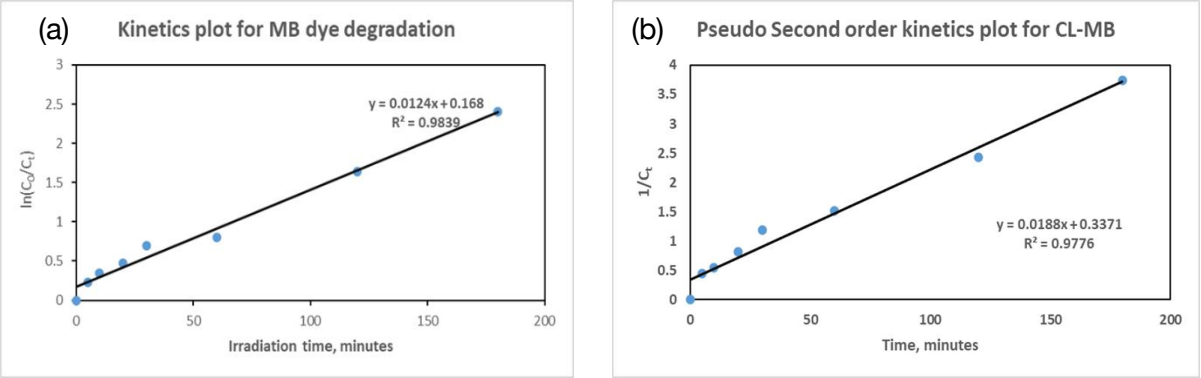


Fig.-6: (a) Kinetics Plot of First Order (b) Kinetics Plot of Second order

Optimization of Degradation Parameters

A three-factor CCD was employed to map the effects of catalyst dosage (A), initial MB concentration (B) and irradiation time (C). Experimental and predicted responses are collected in Table-1. The quadratic model's statistical significance (high F-value, $p < 0.0001$) was validated by analysis of variance (Table-2). Irradiation time emerged as the dominant factor; several two-factor interactions also contributed meaningfully. Predicted and measured values agreed closely, supporting the reliability of the regression equation for process optimization. Three-dimensional response surfaces and contour plots (Fig.-7(a-c)) illustrate the variable interactions. Numerical optimisation identified the conditions catalyst dosage = 0.2 g L^{-1}, initial MB concentration = 30 ppm and irradiation time = 120 min, corresponding to approximately 85.36% degradation. The strong correspondence between predicted and experimental results validates the model. [18-20]

The response data from CCD was used to fit a quadratic model. The following is the equation of the regression line that was obtained for this model:

$$Y = (82.27) + \left(-0.3100A\right) + (-1.01\mathrm{B}) + \left(15.57C\right) + (-2.44\mathrm{AB}) + (0.1912\mathrm{AC}) + (-2.38\mathrm{BC}) + \left(-5.77A^2\right) + \left(-9.60B^2\right) + \left(-28.22C^2\right)$$

Table-1: Experimental and Predicted MB Degradation Efficiencies Obtained from the Central Composite Design.

Run Number	Catalyst Dosage (g/L)	Initial Concentration (ppm)	Time (minutes)	% Degradation Efficiency	
	X	Y	Z	Experimental	Predicted
1	0.1	10	5	20.42	19.79
2	0.2	50	120	72.27	73.02
3	0.2	30	120	85.36	84.37
4	0.3	10	180	60.1	59.96
5	0.1	10	180	55.39	55.30
6	0.3	30	120	76.09	78.35
7	0.2	10	120	74.31	76.53
8	0.2	30	120	85.36	84.37

9	0.2	30	120	85.36	84.37
10	0.2	30	120	85.36	84.37
11	0.2	30	120	85.36	84.37
12	0.2	30	120	85.36	84.37
13	0.2	30	5	35.01	38.48
14	0.2	30	180	70.12	69.61
15	0.1	50	5	28.27	27.43
16	0.1	50	180	52.56	53.41
17	0.3	10	5	25.03	23.67
18	0.3	50	5	22.19	21.54
19	0.1	30	120	78.15	78.85
20	0.3	50	180	48.4	48.29

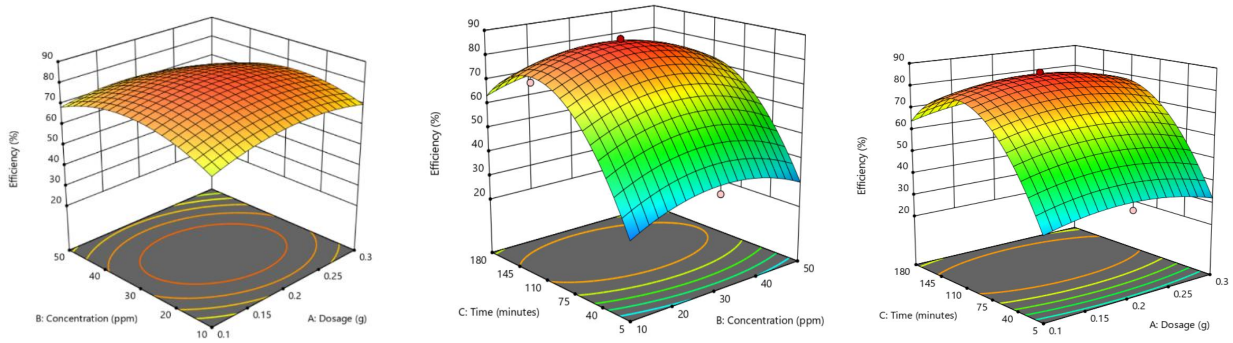


Fig.-7: Analysis of Variance (ANOVA) for the Quadratic Model Describing MB Degradation

Table-2: The Quadratic Model's Statistical Significance (high F-value, $p < 0.0001$) was Validated by Analysis of Variance

Source	*df*	*Sum of Squares*	*Mean Square*	*F-value*	*p-value*	
Model	9	10886.59	1209.62	362.56	< 0.0001	Significant
A (Catalyst loading)	1	0.9565	0.9565	0.2867	0.6041	
B (Initial MB Concentration)	1	10.07	10.07	3.02	0.1129	
C (Irradiation Time)	1	2422.69	2422.69	726.16	< 0.0001	
AB	1	47.82	47.82	14.33	0.0036	
AC	1	0.2983	0.2983	0.0894	0.7711	
BC	1	46.39	46.39	13.91	0.0039	
A^2	1	91.58	91.58	27.45	0.0004	
B^2	1	253.49	253.49	75.98	<0.0001	
C^2	1	1731.91	1731.91	519.11	<0.0001	
Residual	10	33.36	3.34			
Lack of Fit	5	33.36	6.67			
Pure Error	5	0.0000	0.0000			
Total	19	10919.95				

CONCLUSION

The present study demonstrated the successful plant-mediated synthesis of anatase TiO_2 nanoparticles using *Citrus limon* leaf extract and their potential for methylene blue (MB) degradation. Response surface methodology effectively optimized the photocatalytic process, with irradiation time identified as the most influential parameter. The optimum conditions were 0.2g L^{-1} catalyst dosage, 30 ppm initial MB concentration, and 120 min irradiation time, under which an experimental MB degradation of 85.36% was achieved, compared with a predicted value of 84.37%. The degradation followed pseudo-first-order

kinetics with a rate constant of 0.0124 min^{-1} and R^2 = 0.9839. Overall, the plant-mediated TiO_2 photocatalyst shows potential for sustainable treatment of dye-containing wastewater and contributes to SDG-6, particularly Target 6.3.

ACKNOWLEDGMENTS

The authors are thankful to the Department of Chemical Engineering at AUCE(A) and BVRIT for providing experimental facilities for this work.

CONFLICT OF INTERESTS

The authors declare that there is no conflict of interest.

AUTHOR CONTRIBUTIONS

The present work is related to *SDG-6: Clean Water and Sanitation*. All the authors contributed significantly to this manuscript, participated in reviewing/editing and approved the final draft for publication. The research profile of the authors can be verified from their ORCID ids, given below:

Sravani Sameera Vanjarana https://orcid.org/0000-0002-2304-1062
Chitti Babu Nalluri https://orcid.org/0000-0003-1245-1119

Open Access: This article is distributed under the terms of the Creative Commons Attribution 4.0 International License (http://creativecommons.org/licenses/by/4.0/), which permits unrestricted use, distribution, and reproduction in any medium, provided you give appropriate credit to the original author(s) and the source, provide a link to the Creative Commons license, and indicate if changes were made.
Cite this article as: S. S. Vanjarana and C. B. Nalluri, *Rasayan J. Chem.*, Vol.19, Special Issue, 223-231(2026), https://doi.org/10.31788/RJC.2026.19510088

REFERENCES

1. S. Velusamy, A. Roy, S. Sundaram and T.K. Mallick, *The Chemical Record*, **21**, 1570(2021), https://doi.org/10.1002/tcr.202000153.
2. P. Amoatey and M.S. Baawain, *Water Environment Research*, **91**, 1272(2019), https://doi.org/10.1002/wer.1221.
3. I. Khan, K. Saeed, I. Zekker, B. Zhang, A.H. Hendi, A. Ahmad, S. Ahmad, N. Zada, H. Ahmad, L.A. Shah and T. Shah, *Water*, **14**, 242(2022), https://doi.org/10.3390/w14020242.
4. G. Lama, J. Meijide, A. Sanromán and M. Pazos, *Catalysts*, **12**, 344(2022), https://doi.org/10.3390/catal12030344.
5. N. Goodarzi, Z. Ashrafi-Peyman, E. Khani and A.Z. Moshfegh, *Catalysts*, **13**, 1102(2023), https://doi.org/10.3390/catal13071102.
6. H.N.C. Dharma, J. Jaafar, N. Widiastuti, H. Matsuyama, S. Rajabsadeh, M.H.D. Othman, M.A. Rahman, N.N.M. Jafri, N.S. Suhaimin, A.M. Nasir and N.H. Alias, *Membranes*, **12**, 345(2022), https://doi.org/10.3390/membranes12030345.
7. H. Hamrayev, S. Korpayev and K. Shameli, *Journal of Research in Nanoscience and Nanotechnology*, **12**, 1(2024), https://doi.org/10.37934/jrnn.12.1.124.
8. H.R. El-Seedi, R.M. El-Shabasy, S.A.M. Khalifa, A. Saeed, A. Shah, R. Shah, F.J. Iftikhar, M.M. Abdel-Daim, A. Omri, N.H. Hajrah, J.S. Sabir, X. Zou, M.F. Halabi, W. Sarhan and W. Guo, *RSC Advances*, **9**, 24539(2019), https://doi.org/10.1039/C9RA02225B.
9. S.S. Vanjarana, J. Thadaveni, S. Sravya Reddy, B. Rao Are, R. Kethavath, A.K. Kusuma and C.B. Nalluri, *Chemical Product and Process Modeling,* **21(3)**, 311(2026), https://doi.org/10.1515/cppm-2025-0025.
10. A.M. El Shafey, *Green Processing and Synthesis*, **9**, 304(2020), https://doi.org/10.1515/gps-2020-0031.
11. T. Pushpamalini, M. Keerthana, R. Sangavi, A. Nagaraj and P. Kamaraj, *Materials Today: Proceedings*, **40**, S180(2021), https://doi.org/10.1016/j.matpr.2020.08.438.
12. V. Uthiravel, K. Narayanamurthi, V. Raja, S. Anandhabasker and K. Kuppusamy, *Inorganic Chemistry Communications*, **170**, 113327(2024), https://doi.org/10.1016/j.inoche.2024.113327.

13. N.K. Sethy, Z. Arif, P.K. Mishra and P. Kumar, *Green Processing and Synthesis*, **9**, 171(2020), https://doi.org/10.1515/gps-2020-0018.
14. S.B. Jang, S.Y. Yoon, K.T. Wong, C.E. Choong, Y. Yoon, E.H. Choi and M. Jang, *Chemical Engineering Journal*, **467**, 143470(2023), https://doi.org/10.1016/j.cej.2023.143470.
15. R. Mohammadzadeh Kakhki and H. Atarodi Beimorghi, *Journal of Polymers and the Environment*, **33**, 1722(2025), https://doi.org/10.1007/s10924-025-03522-7.
16. M.S.H. Bhuiyan, M.Y. Miah, S.C. Paul, T.D. Aka, O. Saha, M.M. Rahaman, M.J.I. Sharif, O. Habiba and M. Ashaduzzaman, *Heliyon*, **6**, e04603(2020), https://doi.org/10.1016/j.heliyon.2020.e04603.
17. I. Aminu, S.M. Gumel, W.A. Ahmad and A.A. Idris, *American Journal of Analytical Chemistry*, **11**, 47(2020).
18. M.H. Chung, C.T. Wang, J.W. Wang, W.L. Chou and Y.M. Kuo, *Desalination and Water Treatment*, **108**, 144(2018), https://doi.org/10.5004/dwt.2018.21953.
19. K.V. Kumar, K. Porkodi and F. Rocha, *Journal of Hazardous Materials*, **150**, 158(2008), https://doi.org/10.1016/j.jhazmat.2007.09.020.
20. M.A. Behnajady, N. Modirshahla and R. Hamzavi, *Journal of Hazardous Materials*, **133**, 226(2006), https://doi.org/10.1016/j.jhazmat.2005.10.022.
21. N.D. Hai, P.T.M. Huong, N.T. Huu, N.X. Huy, V.T.L. Anh, H.T. Vu, H.V. Doan and M.B. Nguyen, *Advanced Powder Technology*, **36(8)**, 104938(2025), https://doi.org/10.1016/j.apt.2025.104938.
22. M. Aswin, A.R. Jeice and P. Rajaram, *Journal of Crystal Growth*, **666**, 128229(2025), https://doi.org/10.1016/j.jcrysgro.2025.128229.
23. H. Bacelo, S.C.R. Santos and C.M.S. Botelho, *Euro-Mediterranean Journal for Environmental Integration*, **5(3)**, 47(2020), https://doi.org/10.1007/s41207-020-00190-y

[RJC-10088/2026]